

*Araştırma Makalesi- Research Article*

## Change Point Detection Methods for Locating Activations in Functional Neuronal Images

### Fonksiyonel Nöronal Görüntülerde Aktivasyonların Yerini Belirlemek için Değişim Noktası Algılama Yöntemleri

Cemre Candemir<sup>1\*</sup>, Kaya Oğuz<sup>2</sup>

*Geliş / Received: 21/03/2022*

*Revize / Revised: 23/05/2022*

*Kabul / Accepted: 30/05/2022*

#### ABSTRACT

The most common analysis for fMRI images is activation detection, in which the purpose is to find the locations in the brain that respond to specific functions, such as visual processing or motor functions by providing related stimuli as tasks in the experiment. On the other hand, it is also important to detect the instance the activation is triggered. One of the powerful techniques that can analyze the abnormal behavior of any data is change point (CP) analysis. We suggest that CP detection algorithms also can be used to locate the activations in functional magnetic resonance imaging (fMRI) sequences, as well. Our paper presents a two-fold innovative study in that respect. First, we propose to use CP detection algorithms to locate the activations in fMRI signals as a state-of-art topic. Furthermore, we propose and compare a set of change point analysis methods, a regression-based method (RBM), a statistical method (SM), and a mean difference of double sliding windows method (MDSW)) to locate such points. Second, we apply these methods to the fMRI signals, which are acquired from the real subjects, while they were performing fMRI tasks. Proposed methods were applied to three different fMRI experiments with a motor task, a visual task, and a linguistic task. The analysis shows that the methods find activations in accordance with established methods such as statistical parametric maps (SPM). The acquired up to 94 % results also show that the proposed methods can be used effectively to locate the activation times on fMRI time series.

**Keywords – Activation Detection, Activation Instance, Change Point Problem, fMRI, Regression**

#### ÖZ

fMRI görüntüleri için en yaygın analizde amaç, deneyde görevler olarak verilen ilgili uyarılara karşılık beyinde görsel işleme veya motor işlevler gibi belirli işlevlere yanıt veren konumları bulan aktivasyon tespitidir. Öte yandan, aktivasyonun tetiklendiği anın tespit edilmesi de önemlidir. Herhangi bir verinin anormal davranışını analiz edebilen güçlü tekniklerden biri de değişim noktası (DN) analizidir. CP algılama algoritmalarının, fonksiyonel manyetik rezonans görüntüleme (fMRI) dizilerindeki aktivasyonları bulmak için de kullanılabilirliğini öneriyoruz. Makalemiz bu açıdan iki yönlü yenilikçi bir çalışma sunmaktadır. İlk olarak, son teknoloji bir konu olarak fMRI sinyallerindeki aktivasyonları bulmak için CP algılama algoritmalarını kullanmayı öneriyoruz. Ayrıca, bu tür noktaları bulmak için bir dizi değişim noktası analiz yöntemi, regresyon tabanlı yöntem, istatistiksel yöntem ve kayan çift pencere yöntemi öneriyor ve karşılaştırıyoruz. İkinci olarak, bu yöntemleri, fMRI görevlerini gerçekleştirirken gerçek deneklerden elde edilen fMRI sinyallerine uyguluyoruz. Önerilen yöntemler, bir motor görev, bir görsel görev ve bir dilsel görev olmak üzere üç farklı fMRI deneyine uygulandı. Analiz,

<sup>1\*</sup>Corresponding author contact: [cemre.candemir@ege.edu.tr](mailto:cemre.candemir@ege.edu.tr) (<https://orcid.org/0000-0001-9850-137X>)

*International Computer Institute, Ege University, 35100, Bornova, Izmir*

<sup>2</sup>Contact: [kaya.oguz@ieu.edu.tr](mailto:kaya.oguz@ieu.edu.tr) (<https://orcid.org/0000-0002-1860-9127>)

*Department of Computer Engineering, Engineering Faculty, Izmir University of Economics, 35330, Balçova, Izmir*

yöntemlerin, istatistiksel parametrik haritalar (SPM) gibi yerleşik yöntemlere uygun aktivasyonlar bulunduğunu göstermektedir. Elde edilen %94'e varan sonuçlar, aynı zamanda önerilen yöntemlerin fMRI zaman serilerinde aktivasyon anlarını bulmak için etkin bir şekilde kullanılabileceğini göstermektedir.

**Anahtar Kelimeler-** *Aktivasyon Tespiti, Aktivasyon Anları, Değişim Noktası Problemi, fMRI, Regresyon*

## I. INTRODUCTION

It is frequently a matter of interest to know whether there is an existence of change during the analysis of time series. Unexpected abrupt changes or breaks in these series are defined as “change points (CPs).” Since the change point detection (CPD) is an efficient method, it could be applied in various disciplines successfully, such as economy and finance [1], medicine and genetics [2-4], climatology and meteorology [5-7] etc. Because of its applications in these disciplines, various approaches have been proposed to estimate and detect them.

The widely used method in CPD is the Bayesian based approach [8], followed by Hidden Markov Chain [9], maximum likelihood estimation [10], quasi-likelihood estimation [11], regression-based models [12, 13], machine-learning based models [14,15]. Although these methods are frequently used, there are many other algorithms in the literature. A comprehensive survey gives more information in detail [16]. This study extends our previous work [17] that proposed CPD method lays on regression and the statistical features of the data. Apart from the previous study, we have focused on the data acquired from functional magnetic resonance imaging (fMRI) experiments.

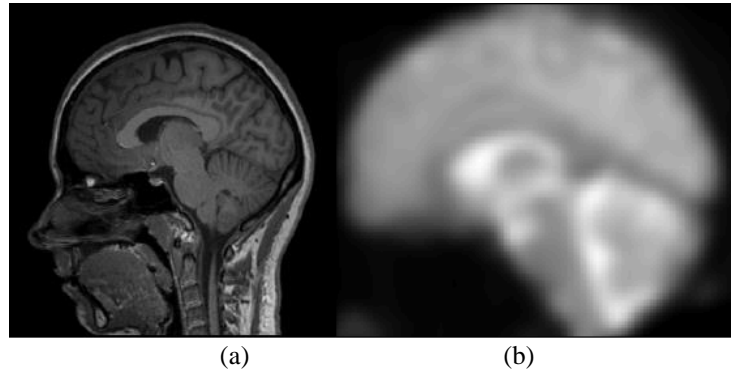


**Figure 1.** Sagittal axis views of (a) the structural image (b) fMRI image.

MRI is a commonly used medical imaging technique to capture the structure of tissues *in vivo*. As the name suggests, it uses a very large magnetic field to align the spin of the hydrogen atoms present in the tissues. The spins are disturbed to tilt them using a signal with specific frequency, called Larmor frequency. This signal is called a pulse, and once it is turned off, the tilted spins start to realign themselves with the magnetic field again. During their alignment, they emit a signal that can be captured by the MRI device. To form an image, the magnetic field must be varied along a slice. Like pixels in an image, the slice contains average signal values from unit volumes, called voxels. This process is repeated for a set of slices, to create a volumetric representation of the tissue [18], as can be seen from a sample mid-slice shown in Figure 1.a. Functional MRI (fMRI) is a mode of MR imaging where the focus is not on the structure of tissues but on the change of blood oxygen levels in the brain, as shown in Figure 1.b. It rests on the idea that the neurons in the brain need energy to fire. The oxygen transported with hemoglobin molecules in the blood stream supplies this energy. The hemoglobin molecules with the oxygen are diamagnetic and they affect the magnetic fields in their vicinity. Once they are free of the oxygen, they become paramagnetic. These inhomogeneities are captured by the scanner in a series of acquisitions, creating a time series for every voxel [18]. This contrast is called the blood oxygen level-dependent (BOLD) [19]. The response to stimulus is called the hemodynamic response and its change in time is called the hemodynamic response function (HRF) [20]. The structure of the HRF is given in Figure 2. The time series of the functional images are modeled with the convolution of the given stimulus and the HRF. The fMRI experiments make use of these time series to analyze brain functions.

The most common analysis is activation detection, in which the purpose is to find the locations in the brain that respond to specific functions, such as visual processing or motor functions by providing related stimuli

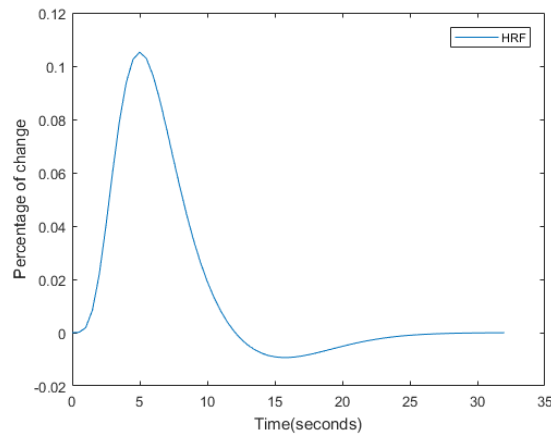


**Figure 2.** The hemodynamic response function generated by SPM's `spm_hrf()` method..

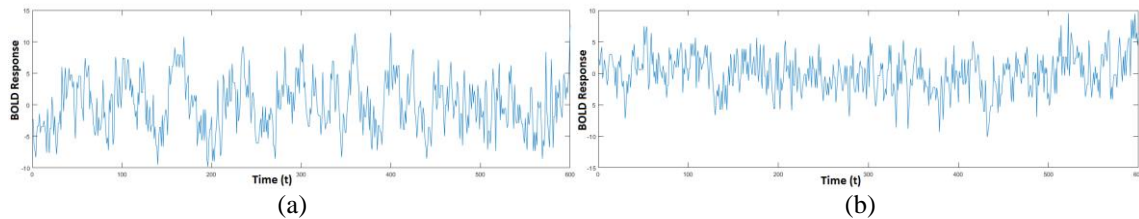


**Figure 3.** Time series of (a) a non-active voxel (b) an active voxel. Here, x-axis denotes the time, whereas y-axis denotes the BOLD response along the time.

as tasks in the experiment. The activated voxel is expected to respond with the HRF, which shows an increase in the BOLD signal. Figure 3 shows a sample time series for a non-active and an active voxel. Another analysis is resting state analysis, where instead of tasks the subject lies still, and the data is analyzed for correlations of time series in different regions.

Besides the activation detection, finding the timing of the activations is also another important question and traditional activation detection methods could not reveal such points. The timing of the activations on the fMRI signals should be consistent with the timing of given stimuli. Delays or non-activations may include crucial information about some psychological or physical abnormalities and such instances should be located as they occurred. In this study, we propose the model the activation instances as *change points* and suggest to use CPD algorithms in fMRI signals to find the locations of the activations which occurs with the given stimuli along the time. The paper presents a multi-fold innovative study in that respect. Contributions can be listed as follows:

- We propose to use CP detection algorithms to model the activations as if they are the abnormal behaviors of the fMRI signal.
- We propose and compare a set of change point analysis methods, a regression-based method (RBM), a statistical method (SM), and a mean difference of double sliding windows method (MDSW)) to locate such points.
- We apply these methods to the fMRI signals, which are acquired from the real subjects, while they were performing fMRI tasks. Proposed methods were applied to three different fMRI experiments with a motor task, a visual task, and a linguistic task in this context.

The following section discusses the related work on the change point problem and activation detection in fMRI. The third section is about the acquisition and the preprocessing of the fMRI data. Details of the proposed methods are presented in Section IV and the results are given in Section V. Discussions are presented in Section VI.

## II. RELATED WORK

Change point problems could be categorized in 'estimation' and 'detection' subcategories. The first step in estimation is to investigate whether there is a change in the data or not. If there is no prior knowledge that the data contains any changes, hypothesis tests are used to examine the existence of the CP. Here,  $H_0$ (null hypothesis) shows that the data set has a homogeneous structure, while  $H_1$ (alternative hypothesis) points out the presence of at least one such point in the data. In this study, we seek the locations of the activation points and due to the structure of the fMRI task that will be detailed in Section III, it is known that there is at least one CP.

The more complex part of CP problem is detection. The detection problem searches for the locations of CPs that are known to exist somewhere in the data. One of the fundamental methods named Cumulative Sum (CUSUM) is a very powerful and efficient statistical method and can be adapted in a wide variety of problems such as financial trading and anomaly detection [21,22]. Besides CUSUM and its hybrid variations, Shiryaev-Roberts (SR) is also a powerful and important method to detect such points [23]. The robustness of the SR method on change detection problems has been widely discussed in the study of Du et.al. [24].

In CPD problems, most commonly used methods are Bayesian based. The main idea of the Bayesian methods rests on the posterior probability and the prior probability comparisons. An inference that shows whether there is a significant change or not is done by evaluating and differentiating the probability densities together. Bayesian based methodologies can be classified as offline and online. Offline approaches handle the data set as a batch and identify the locations of the points by looking back to the whole data set. Many of the Bayesian studies work offline on a fixed size data [25-27]. On the other hand, online approaches work on a sequential data and aim to detect the locations of the CPs as soon as possible after they occur. Online algorithms must update themselves quickly with every new observation stream. The effectiveness of the online algorithm depends on the ability to detect the CPs by the number of the least observed data in the new observation stream. One of the leading studies of Bayesian online change point detection (BOCPD) is discussed in [28]. Generalization of the BOCPD method which learns the parameters from the data model is suggested to solve the dependencies of the user dependent parameters [29]. Hierarchical Bayesian model [30], Gibbs sampling [31], Schwartz Information Criterion (SIC) [32], Markov Chain Monte Carlo (MCMC) [33], dynamic programming [34] and its hybrid applications with particle filters [35,36] are some other approaches that are based on Bayesian methodology.

Another widely used and referenced CPD methodology is Maximum Likelihood Estimation (MLE). The main idea behind the MLE is to be able to estimate the parameters of given distributions from the stream of the observed data. It aims to find the set of the parameter values that maximizes the likelihood function. MLE is used to evaluate the distributions before and after a point and infers a CP by considering these distributions of time. Using MLE in CP problems was introduced in 1970's [37, 38] and one of the milestones of this methodology belongs to the study discussed in [39] which suggests the generalization of single CPD using MLE and Expectation-Maximization (EM) in multipath CP problems. Empirical Likelihood Ratio (ELR) [40], Quasi Maximum Likelihood (QML) [41], Quasi Gaussian Likelihood (QGL) [42] are also some different methodologies that are based on the MLE.

Besides the methodologies mentioned above, another suggested methodology is using the regression model to detect the CPs. If data is stationary, the regression line is expected to have a constant slope. If there are major changes in the slope, it implies that the regression line is broken sharply at one or more points. The moments that the break occurs are defined as the CPs. One of the important studies that models the unknown CP dividing the regression line into two parts is presented in [43]. This method is insufficient because it is based on the knowledge that there is only one CP in the data. In the case where there are more than one, the exact number of the changes should be known. Furthermore, there are many hybrid studies which use the regression-based and other algorithms together. This methodology can be used to infer whether there is a change or not with using the MLE [44] and test the changes using a recursive residual model in multiple regression [45]. Regression is also used with combining other methodologies such as likelihood ratio tests [46], hybrid usage of SIC and binary segmentation [47], generalized MLE in logistic regression [48], penalized likelihood in piecewise regression [49] and genetic programming in sliding window symbolic regression [50].

### III. MATERIALS AND PRELIMINARIES

#### A. fMRI Experiments and Activation Detection

As introduced earlier, functional magnetic resonance imaging aims to capture the change in oxygen levels in the blood while the subject is doing an fMRI task to locate the brain regions responsible for the performing functions. A basic fMRI experiment to locate the motor functions in the brain, for example, contains two tasks; one task where the subject is asked to tap their fingers in both hands, and another task where they are asked to lie still. Since the brain always in activating, it is a challenging situation, therefore, two different states are needed where one state includes the sought function and the other does not. In such an experiment, the regions responsible for the motor functions will have an increase in the BOLD contrast during the finger tapping task. This type of experiment is called a block design experiment.

Activation detection in fMRI studies is an important field that has been studied extensively. One of the first proposed activation detection methods is the subtraction method, as detailed in [51]. The experiment in the paper is a typical finger tapping task where the subjects are either at rest, or are tapping their fingers. This method takes the average volumes of the two tasks in the experiment and subtracts them from each other. The activated regions are located by the voxels with highest values. The paper also discusses the use of correlation between the voxel signals and the square wave form of the design of the experiment. The square wave form is obtained by setting the instances while the subject is at rest as zeros, and the instances while the subject is tapping as ones. This signal is also called a boxcar signal because of its shape. The correlation between this expected square wave form output and the received voxel signal reflect the correlation of voxel responses to the motor functions in the experiment.

While the correlation and the general linear model (GLM) which will be discussed in detail shortly dominate the literature, there are several other methods for detecting the activation in fMRI experiments, such as the application of parametric and nonparametric statistical tests [52], statistical tests with filters [53,54], cross-correlation analysis [55], statistical analysis in wavelet domain [56], principal component analysis (PCA) [57], Bayesian based approach on Relevant Vector Machines (RVM) [58], Bayesian multilevel models [59], independent component analysis (ICA) [60], support vector machines (SVM) [61] and regression based method [62] as well.

Statistical Parametric Maps (SPM), a widely used tool based on the GLM, is used to find active voxels in fMRI images [63,64]. The GLM is based on the equation given below with the (1),

$$Y = X\beta + U \quad (1)$$

Here,  $Y$  contains the BOLD values of voxels,  $X$  comprises of the variables effecting the fMRI task. GLM estimates the  $\beta$  matrix which shows how much each variable affects the signal.  $U$  is the error matrix that is assumed to be independent and identically distributed. After the  $\beta$  values are estimated, a contrast vector can be used to test for the effects inherent in the experiment.

The GLM approach is used extensively in both practice and the literature. The other software packages which implement the method to help both clinical and research experiments are FSL and AFNI.

Nevertheless, GLM may be limited when modeling the state-related single epoch paradigms such as emotional states, anxiety and social exclusion [65]. GLM is interested in the response given to the functions in the tasks. It uses the design matrix with the contrast vector to find the statistically significant voxels. Any function that is not in the task is not sought, and therefore cannot be located. This stops GLM from exploring the signals for activations that are not in a task. It does not allow its users to estimate the instance an emotional state triggers an activation. Although it is a powerful and an efficient method for analyzing the fMRI data, this constitutes as one of the limitations of the GLM model.

The methods discussed so far are effective, but they are used to find the activated regions in the brain. In addition to the activated regions, the instance the activation triggered is also an important question. So, in an additive manner to the GLM, it is required to know the timing and the magnitude together. However, it is a complicated problem and it is harder to specify the location of the activation point along the time, for both single subject and multiple subjects due to the subject variabilities of the BOLD response. Moreover, there may be more than one activation point according to the fMRI task, but some subjects may not show any response. There are relatively fewer studies for the detection of the activation points of fMRI data in the literature. The most important

studies on this problem use multi-subject extension of the exponentially weighted moving average (EWMA) [66] and hierarchical EWMA (HEWMA) [65]. Both models are applied on a state-related fMRI study related with anxiety. Another study is performed on a visual fMRI task and propose a computational framework in correlation networks [67].

In this study, we propose to find the timing of the activations of the subject, which is referred to as a “change point”, from fMRI signal along the time series. Detection of the exact timing of the activation can be handled as a CPD problem in time series. Thus, we extended our previous study that proposed CPD algorithms based on regression and statistical properties on well-log data set.

### ***B. fMRI Data Acquisition and Preprocessing***

The proposed methods are evaluated using three different data sets. Two of the data sets are collected using the Siemens 3T Magnetom scanner at the Ege University. The third data set is acquired using a SignaHDxt 1.5T scanner at the Brain Research Imaging Centre [68]. The subjects in the experiments are healthy volunteers. The task details are discussed in the following subsection.

fMRI data requires a set of processing stages due to artifacts that arise from the scanner and subjects. It is difficult for subjects to stay still during fMRI experiments that can take up to 30 minutes. Physiological functions such as breathing, and the heart rate also cause involuntary movements that can create artifacts. Scanner related artifacts may be caused by the temporal resolution, such as system noise, and spatial resolution such as radio-frequency artifacts. These artifacts should be eliminated in the preprocessing stage.

Preprocessing stage consists of several steps. The main objectives during preprocessing are to align the images to a standard space and to remove the noise as much as possible so that the validity of the group analysis is increased while the physiologic and scanner related artifacts are minimized. The preprocessing of the fMRI data is done with the SPMv12. SPM takes the first image as the reference volume and realigns the other images of the subject with rigid body transformations [69]. The realigning process also slices the volume again so that it matches the reference volume voxel by voxel. The average value for each voxel is calculated in this step, which results in a mean image.

Since the brain is modeled of multiple slices, there may be time differences between the slices during the fMRI scan. To handle this issue, slice timing is done to shift the time of each voxel to the same time course as if they have been scanned simultaneously at the same time. After all slices are aligned and synchronized in time, SPM registers the structural scan with the mean image that acquired in the realigning step [70].

In the segmentation step, brain is cleaned out from the surrounding tissues. These structures are classified according to the tissue probability map based on the knowledge of being specific types of tissue at specific locations. The structural image is also standardized to a global standard space during segmentation (MNI space) [71]. After this step, all images are registered to the MNI space and by this way, the analysis can be generalized among the subjects. Smoothing is the final preprocessing step which convolves the images with a Gaussian kernel to suppress the noise and artefacts caused by the residuals transferred from the previous steps.

### ***C. Visual Task Data Set***

This data set is acquired from a block design experiment to locate the regions responsible for visual processing. The first block contains the resting task, where the subject lies still looking at a blank screen for thirty seconds. The second block contains the visual task, where the subject is shown 6 successive photographs of random people from the study by [72] for 6 seconds each, followed by one second of blank screen. This second block takes 40 s to complete. These blocks are repeated for 12 times. The acquired image volumes consist of 36 slices, where each slice has a size of 64 by 64. The voxel size is 3x3x3.74 mm. The repetition time for the scans is 3 s, with an echo time of 30ms and a flip angle of 90 degrees. This data set is referred as DS1 throughout the manuscript.

### ***D. Motor Task Data Set***

This is a *finger tapping* experiment to locate the regions related to motor functions of the brain. It is a block design experiment that contains two tasks. The resting task requires the subject to lie still without any movement for sixty seconds. During the tapping task, they are instructed to tap their fingers on their both hands for 60 seconds. The tapping is self-paced. These tasks are repeated for 12 times. The repetition time for the scans is 2 seconds with an echo time of 30 ms and flip angle of 90 degrees. The acquired volumes have 23 number of

slices with a matrix of size 64x64. The voxel size is 3x3x3 mm. This data set is referred as DS2 throughout the manuscript.

### **E. Linguistic Task Data Set**

This is a verb generation experiment for mapping the regions responsible for language in the brain. The subjects are asked to generate verbs according to the instructions they hear. The repetition time for the scans is 2.5 seconds, with an echo time of 50ms and flip angle of 90 degrees. There are 30 slices per volume and a matrix of size 64x64. The voxel size is 4x4x4mm [68]. This data was obtained from the OpenfMRI database. Its accession number is ds000114 (<https://openfMRI.org/dataset/ds000114/>). It is referred as DS3 throughout the manuscript.

### **F. Voxel Selection**

All data sets are preprocessed using SPM, as mentioned in Section III.B. Then, they are analyzed using SPM which uses the general linear method. After this process, three voxels from each data set have been chosen; the first one is the statistically most active voxel, one is randomly chosen from the activated areas, and the third one is the least active voxel. Instead of using synthetically generated BOLD signals where the activations are known, signals from real subjects that have been detected as active by SPM and GLM have been chosen, since they are commonly used methods both in research and clinical operation.

## **IV. METHODS**

### **A. Outlier Detection**

The proposed methods make use of outlier detection methods to locate the exact CPs in the BOLD signals. A practical way to detect outliers is using their position from the mean value  $\mu_x$  of the given signal  $X$ . The threshold distance is determined by multiplying the threshold coefficient  $p$  by the standard deviation  $\sigma_x$ . The generally used threshold coefficient value is  $p=3$ . The  $p$  value marks other time points as outliers which located outside the interval  $(\mu_x - p \sigma_x, \mu_x + p \sigma_x)$ .

Instead of using the standard deviation, another suggested method is to the use of the median absolute deviations (MAD). MAD is defined as  $MAD = median(|X - median(X)|)$ . For normal distributions, MAD is used with a scale factor  $k$  computed with the equation (2)

$$k = 1/(\Phi^{-1}(3/4)) \approx 1.4826 \quad (2)$$

Here,  $\Phi$  is the opposing of the quantile function. The  $p$  coefficient is set to 3 and elements outside the interval  $(\mu_x - p \times MAD(X), \mu_x + p \times MAD(X))$  are marked as outliers. Grubb's method may also detect the outliers as well [73]. Grubbs' method discovers one outlier at a time, removes it, and repeatedly re-evaluates the remaining points until no more outliers are found. Some of the remaining outliers may be statistically lost as a result of the elimination between repetitions.

### **B. Regression Based Method (RBM)**

The activation in the BOLD signal is defined by a relative increase in the task that contains the sought function. This relative increase creates a change point which may be detected by the regression analysis of a window sliding through the signal. The detected change point represents the activation instance of the voxel. The regression line of such a window could be expressed as  $Y = mx + b$  where  $m$  is the slope and  $b$  is the y-intercept. The relative increase of the BOLD signal is expected to create a shift in the positive direction in the given BOLD time series. This will result in an increase in  $m$  signaling the location of the change, as can be seen in Figure 4. This location, however, points out somewhere in a window of a fixed interval, and further processing is required for finding the point where the change occurs.

RBM analyzes the given time series  $X$  with a window size  $w$ , in fixed intervals defined with a step size of  $s$ . This method, known as the sliding window, estimates the slope  $m$  for each window using linear regression with the least squares method and gives the slope vector  $M$ . The parameters  $w$  and  $s$  depend on the time sequence of the fMRI data and should be set by trial and error.

$M$ , the acquired slope vector, is then examined for outliers, which reflect the windows that depart the most from the mean and thus are potential intervals for change points. Outliers can be detected using any of the statistical approaches outlined in Section IV.A. Outlier identification can be used to identify outliers in a series of points. The interval containing the change point is chosen as the one with the greatest absolute value of  $m$  among them. This interval's first derivative is calculated, and the global maximum is chosen as the CP because it reflects the maximum change.

### C. Statistical Method (SM)

CPs in the data can be determined using statistical parameters such as the mean. The mean of the data prior to the candidate CP considerably differs from the mean of the data following the candidate CP. The method specifies a window width ( $w$ ), which sets the entry numbers analyzed preceding and following the candidate to discover this process. The window size  $w$  is determined by the nature of the fMRI data and should be determined via observation and experimentation.

The initial step of the algorithm is taking the  $(w + 1)^{th}$  index and computes the mean of the preceding window  $w$  and gets the mean  $\mu_1$ . It obtains  $\mu_2$  by computing the mean of the window that starts at index  $w + 2$ .  $\mu_1$  indicates the change magnitude for the related time point. The outliers for vector  $D$ , which contains the mean differences for all points, are the candidates for change points. As before, any of the methods in Section IV-A can be used. Like the RBM, sequential points could be labeled as outliers. Since the activation will cause an increase in the BOLD signal, the point with the greatest positive mean difference is chosen as the CP.

### D. Mean Difference of Double Sliding Windows (MDSW)

As opposed to the SM that considers the difference in the mean of two windows before and after the candidate point, Mean Difference of Double Sliding Windows uses the two windows of different sizes starting from the candidate point. The algorithm uses windows of size  $s_1$  and  $s_2$  to compute two mean values  $\mu_1, \mu_2$  starting from the first index in the data. The convention is to set the second windows size to be greater than the first. As the algorithm iterates through the points in the data, the difference of  $\mu_2 - \mu_1$  is stored on the vector  $M$ . The outliers in this vector are located using the outlier methods discussed in Section IV-A. Similar to other methods, a series of differences can be set as outliers. Since the HRF will result in an increase in the BOLD signal, the greatest positive value among these consecutive outliers is selected as the CP.

## V. RESULTS

### A. Testing Conditions

The algorithms are tested by varying the values for the outlier threshold,  $t$ , sliding window width ( $w$ ), and the step size ( $s$ ). The outlier detection is done using the median absolute deviations (MAD) as detailed in Section IV-A. In a few cases, the outliers are detected by their distance to the mean. These cases will be discussed in the following section. The threshold parameter is tested with the values 1, 2 and 3 for both MAD and mean outlier detection methodologies for all methods.

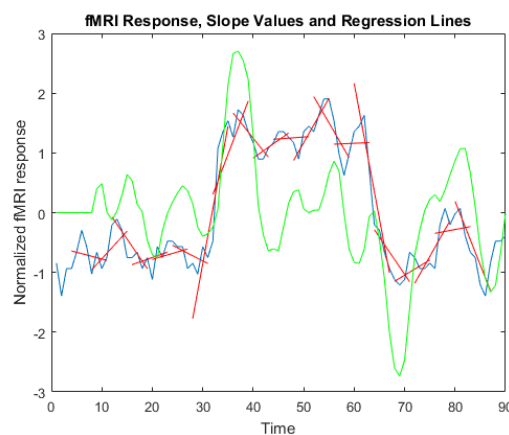


**Figure 4.** The fMRI response is shown in blue, the slope vector  $M$  is shown in green, and the regression lines for the windows are shown in red [74].

The second parameter is the window size. The repetition time for the functional image acquisition varies from 2 seconds to 3 seconds. Considering the time for the hemodynamic response function to peak, we have set the window size to be at least 4 scans, which varies from 8 to 12 seconds. As the stimulus continues the convolution of the signal and the HRF results in a signal similar to the one shown in Figure 3.b. Although values for the peak magnitude and the latency to start peaking may vary, the choice of window size should be large enough to contain the peak which takes around six to eight seconds after the stimulus is given.

The third parameter is the step size of the sliding window. If the step size is greater than the window, the algorithms can skip change points. The combinations where the step size is greater than the window size are discarded.

Not every parameter is needed for every method. The RBM is tested with the parameters  $w$ ,  $t$  and  $s$  (window, threshold and step size respectively). The parameter  $w$  is tested with the values 4, 6, 8, 10 and 12. The

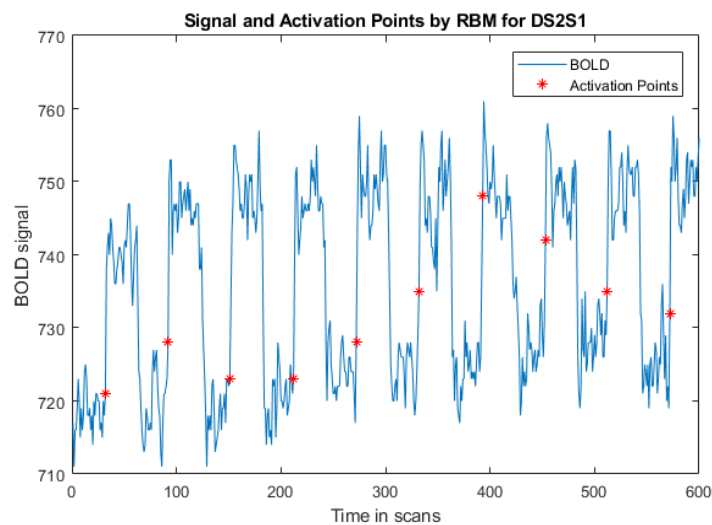


**Figure 5.** The plot shows the BOLD signal for the most activated pixel in the second data set, marked as DS2S1. The activation points are shown as red stars.

step size parameter is adjusted to 1, 4 and 8. SM is evaluated with the parameters  $w$  and the threshold  $t$ . These parameters are also set to the same values used for RBM. Finally, the mean difference of double sliding windows (MDSW) is tested with the  $t$ ,  $s$  and two window sizes  $w_1$  and  $w_2$ . Both threshold and step size parameters are run with the same values used for RBM and SM. The double sized window size is selected as [4, 6], [6, 9], [8, 12], [10, 15] and [12, 18]. The second window is set as one half larger than the first one.

### B. Evaluation and Results

The algorithms are evaluated by their precision of locating the expected activation instances. In block design experiments, such as the ones we are considering, the stimuli are given at fixed intervals. The algorithms return the change points as the activation instances they have detected (see Figure 5.). For an expected activation at instance  $a$ , the algorithm will detect a change point at instance  $c$ . This instance is expected to be as close as possible to instance  $a$ . However, we are not accepting any instance that is further away from the duration  $d$  of the task. The score  $sc$  of the algorithm, which is defined with the equation (3), is based on the ratio of the distance between the change point at  $c$  and the activation instance at  $a$ , to the duration  $d$  of the task.

$$sc = \frac{1}{\max(n_a, n_c)} \sum_{i=1}^{n_a} \sum_{j=1}^{n_c} \max\left(\frac{(d - |a_i - c_j|)}{d}\right), \text{ for } |a_i - c_j| < d \quad (3)$$

As shown in Equation (3), the maximum among the detected change points that are within the task duration are summed to compute the score for the expected activation point. The algorithm may return more change points than the expected activation points. In that case, the score uses the maximum number of change points for normalization ( $\max(n_a, n_c)$ ). In the case that the algorithm detects fewer number of change points, then the

expected number of activation points are used for normalization. If the algorithm can detect all the activations precisely when they are expected, then it gets the maximum score of 1.

The results for the datasets DS1, DS2, and DS3 are given in Table 1. The signals for each dataset are selected among the most active voxels, which are detected by SPM, according to the activation regions for each fMRI task. To save the space, only the highest-ranking optimal parameters are listed in the table.

**Table 1.** Best detection scores and optimal parameters for the datasets DS1, DS2, and DS3.

	RBM		SM		MDSW	
	Parameters	Score (sc)	Parameters	Score (sc)	Parameters	Score (sc)
DS#1	$s = 4, w = 10, t = 1$	0.63	$w = 6, t = 1$	0.577	$w = 12, s = 1, t = 1$	0.57
DS#2	$s = 1, w = 8, t = 2$	0.94	$w = 8, t = 2$	0.94	$w = 8, s = 1, t = 2$	0.84
DS#3	$s = 1, w = 8, t = 1$	0.82	$w = 8, t = 2$	0.81	$w = 6, s = 1, t = 1$	0.83

To be able to explore the effect of the parameter selection for the proposed methods, also the methods RBM, SM, and MDSW were run with different parameter sets. The results for the parameter changes are given in Table 2. Here, it is shown how the outcome score will be affected when at least one parameter is kept constant and the others are changed. For example, for DS1, when the step size ( $s$ ) and window width ( $w$ ) keep constant, the changes in the threshold ( $t$ ) parameter from 1 to 2 result a prominent decrease in the detection score ( $sc$ ) in RBM. On the other hand, when the results are examined for DS2, the changes of two parameters together,  $s$  and  $w$ , while the  $t$  value keeps constant at  $t = 2$ , also affects the  $sc$  score dramatically, from 0.94 to 0.85. For the SM, the parameters are  $w$  and  $t$ , and the results are evaluated for the effect of parameter change while a parameter is kept the same. The results show that the selected window width affects the resulting detection score more than the threshold parameter. And finally, when analyzing the MDSW method, it can be observed that increasing the step size results in decreasing the detection score from 0.84 to 0.79 while  $w$  and  $t$  are constant. The possible reason is being skipped the candidate change points when getting larger the step size. The other observation is that when  $t$  keeps the same, decreasing the parameter  $w$  and increasing the parameter  $s$  do not affect the detection score significantly. Thus, any changes in the  $w$  and  $s$  parameter should be done in the opposite ways at the same time.

**Table 2.** Effects of the parameter selection on the detection score results for the datasets DS1, DS2, and DS3.

	RBM		SM		MDSW	
	Parameters	Score (sc)	Parameters	Score (sc)	Parameters	Score (sc)
DS#1	$s = 4, w = 10, t = 1$	0.63	$w = 6, t = 1$	0.577	$w = 12, s = 1, t = 1$	0.57
	$s = 4, w = 10, t = 2$	0.55	$w = 8, t = 1$	0.575	$w = 12, s = 1, t = 2$	0.54
	$s = 1, w = 12, t = 1$	0.57	$w = 6, t = 2$	0.568	$w = 10, s = 1, t = 1$	0.56
DS#2	$s = 4, w = 8, t = 2$	0.94	$w = 8, t = 2$	0.94	$w = 8, s = 1, t = 2$	0.84
	$s = 4, w = 12, t = 2$	0.93	$w = 10, t = 2$	0.84	$w = 8, s = 2, t = 2$	0.79
	$s = 1, w = 10, t = 2$	0.85	$w = 8, t = 1$	0.92	$w = 10, s = 2, t = 1$	0.81
DS#3	$s = 1, w = 8, t = 1$	0.82	$w = 4, t = 1$	0.89	$w = 6, s = 1, t = 1$	0.83
	$s = 1, w = 12, t = 1$	0.75	$w = 8, t = 1$	0.71	$w = 8, s = 1, t = 1$	0.655
	$s = 4, w = 8, t = 2$	0.72	$w = 10, t = 1$	0.61	$w = 6, s = 2, t = 1$	0.653

Since the nature of the problem is highly dependent on fMRI data, this point also constitutes one of the main restrictions for comparing the other methodologies. Accurate comparisons can only be made using signals from the same data set. For the effectiveness of the proposed methods according to the well-known methodologies, in the last step, RBM, SM, and MDSW are compared with the performance of the Bayesian-based sequential change-point detection approach [34]. The dynamic Bayesian algorithm has been implemented and run with the DS1, DS2, and DS3 activation signals. For the Bayesian approach, the parameters are as follows:  $\{N = 15, d = 20, k = 0.001\}$  which indicates the maximum number of change points, the minimum distance between adjacent change points, hyperparameter for the prior on the regression coefficient, respectively. For evaluating the results, change points have been chosen as the points whose posterior probability is bigger than the  $p > 0.40$  for DS1 and DS3, and  $p > 0.80$  for DS2 (here, it has been taken into account the fMRI task design). According to the comparative results shown in Table 3, the proposed methods are slightly over from the Bayesian approach in detection performance for DS2 and DS3. For the DS1, the performance of the Bayesian is not strong as the proposed methods.

**Table 3.** Comparative results of the methods with Bayesian Method for DS1, DS2, and DS3.

	RBM	SM	MDSW	Bayesian [34]
DS#1	0.63	0.577	0.57	0.44
DS#2	0.94	0.94	0.84	0.934
DS#3	0.82	0.81	0.83	0.826

## V. DISCUSSION

The results show that the algorithms can locate activations using the change point detection methods. However, the parameters affect the results and they need to be tuned in accordance with the subjects and the tasks. The most obvious factor is the threshold used for the outlier detection in the resulting vectors. If the threshold increases, the reliability of the points as a change point also increases. However, it reduces the number of detected change points, and hence the activation points which skips some of the subtle activations.

Outlier detection is also affected by the choice of the method. While MAD approach is more robust, it has the same conclusion as having a high threshold value; the reliability increases but some of the activations are lost. Reducing the step size increases, the computation time, albeit not so much for an fMRI experiment, but increases the precision because it is less likely for the method to miss an activation point because of the sliding window. As can be seen from the tables, most of the results have a step size of 1, where the data is continuously checked for change points. The window size, as mentioned earlier, mostly depends on the HRF peak time. This changes from subject to subject, and even from region to region in a single subject.

Among the methods, the regression-based method outperforms the others. However, it is computationally more expensive. The slope computed by the regression is a good measure for detecting the increase in the BOLD signal, pointing the algorithm to the correct instances.

The signals used have already been identified as active by the SPM method, and this begs the question about the necessity of the proposed methods. SPM and other related methods look for signals that are correlated with the fMRI experiment. The time the stimulus given is fixed and an activation is expected then and there. While they can tolerate latencies, they need the structure of the experiment to infer some results. The proposed methods do not need any structure to be given to find the activation points. This can be used in many different scenarios, such as when analyzing resting state data where there is no task to base the structure on, or for detecting when the emotional state of the subject has changed.

Finally, it could be also mentioned about the limitations of the study. Besides the abovementioned points, this study is highly data-driven and parameter-dependent in its nature. Additionally, there are also external affecting factors, such as the complexity of the given fMRI task, detected activation regions according to the task, inter-subject and intra-subject variations etc. All these factors should be considered while applying the methods on a BOLD signal. If fMRI datasets can be sufficiently multiplied and diversified, parameter dependency can be reduced through methods such as deep learning. In this context, it is planned to constitute the future works in this manner for detecting the activation times in BOLD signals.

## REFERENCES

- [1] Sargun, D., & Koksal C.E. (2021). "Robust Change Detection via Information Projection," IEEE Journal on Selected Areas in Information Theory, 2(2), 774-784.
- [2] Kass-Hout T.A., Xu, Z., Mc Murray, P., Park, S. Buckeridge, D.L. Brownstein, J.S., Finelli, L., & Groseclose, S.L. (2012). "Application of change point analysis to daily influenza-like illness emergency department visits," J. Am. Med. Inform. Assoc. JAMIA, 19(6), 1075–1081.
- [3] Zhang, N.R., Siegmund, D. O., Ji, H., & Li, J. Z. (2010). "Detecting simultaneous change points in multiple sequences," Biometrika, 97(3), 631–645.
- [4] Feber, A., Guilhamon, P., Lechner, M., Fenton, T., Wilson, G.A., Thirlwell, C., Morris, T. J., Flanagan, A.M., Teschendorff, A.E., Kelly, J.D., & Beck, S. (2014). "Using high-density DNA methylation arrays to profile copy number alterations", *Genome Bio.*, 15(2), R30.
- [5] Ruggieri, E., Herbert, T., Lawrence, K. T., & Lawrence, C. E. (2009). Change point method for detecting regime shifts in paleoclimatic time series: Application to  $\delta^{18}\text{O}$  time series of the Plio-Pleistocene, *Paleoceanography*, 24(1), PA1204.
- [6] Gallagher, C., Lund, R. & Robbins, M., (2012). Change point detection in daily precipitation data, *Environmetrics*, 23(5), 407–419.

- [7] Perreault, L., Bernier, J., Bobée, B., & Parent, B. (2000). Bayesian change-point analysis in hydrometeorological time series. Part 1. The normal model revisited, *J. Hydrol.*, 235(3), 221–241
- [8] Mostafa, A. A., & Ghorbal, A. B. (2011). Bayesian and Non-Bayesian Analysis for Random Change Point Problem Using Standard Computer Packages, *Int. J. Math. Arch.*, 2(10), 1963–1979.
- [9] Elliott, R. J., and Siu, T. K. (2014). Filtering and change point estimation for hidden Markov-modulated Poisson processes, *Appl. Math. Lett.*, 28, 66–71
- [10] Gazor, S., Derakhtian, M., & Tadaion, A.A. (2010) Computationally Efficient Maximum Likelihood Estimation and Activity Detection for M-PSK Signals in Unknown Flat Fading Channels, *IEEE Signal Proc. Letters*, 17(10), 871–874.
- [11] Bardet, J.-M., Kengne, W., & Wintenberger, O. (2012). Multiple breaks detection in general causal time series using penalized quasi-likelihood, *Electron. J. Stat.*, 6, 435–477.
- [12] Toms, J. D., & Lesperance, M. L. (2003). Piecewise Regression: A Tool for Identifying Ecological Thresholds, *Ecology*, 84(8), 2034–2041.
- [13] Wu, W. B., Woodroffe, M., & Mentz, G. (2001). Isotonic Regression: Another Look at the Change Point Problem, *Biometrika*, 88(3), 793–804.
- [14] Hu, S., & Zhao, L. (2015). A Support Vector Machine Based Multi-Kernel Method for Change Point Estimation on Control Chart, *IEEE Int'l Conf. on Systems, Man, and Cybernetics*, Hong Kong, China, 492–496.
- [15] Kazemi, M. S., Kazemi, K., Yaghoobi, M. A. & Bazargan, H. (2016). A hybrid method for estimating the process change point using support vector machine and fuzzy statistical clustering, *Appl. Soft Comput.*, (40), 507–516
- [16] Aminikhanghahi, S., & Cook, D. J. (2017). A survey of methods for time series change point detection, *Knowl. Inf. Syst.*, 51(2), 339–367.
- [17] Candemir, C., & Oğuz, K., (2017). A Comparative Study on Parameter Selection and Outlier Removal for Change Point Detection in Time Series, *IEEE European conf. on Elec. Engineering and comp. Sci. (EECS)*, Bern, Switzerland, doi: 10.1109/EECS.2017.48
- [18] Deichmann, R. (2009). Principles of MRI and Functional MRI, in *fMRI Techniques and Protocols*, Humana Press, Totowa, NJ, 3–29.
- [19] Ogawa, S., Lee, T. M., Kay, A. R., & Tank, D. W. (1990). Brain magnetic resonance imaging with contrast dependent on blood oxygenation, *Proc. Natl. Acad. Sci. U. S. A.*, 87(24), 9868–9872.
- [20] Handwerker, D. A., Ollinger, J. M., & D'Esposito, M. (2004). Variation of BOLD hemodynamic responses across subjects and brain regions and their effects on statistical analyses, *NeuroImage*, 21(4), 1639–1651.
- [21] Xin L., Yu P.L.H., & Lam K. (2013). An Application of CUSUM Chart on Financial Trading, *9<sup>th</sup> Int'l Conf. on Computational Intelligence and Security*, 14-15 December, China.
- [22] Callegari C., Pagano M., & Giordiano S., (2017). CUSUM-based and entropy-based anomaly detection: An Experimental comparison, *8<sup>th</sup> Int'l Conference on the Network of the Future*, 22-24 Nov., London
- [23] Polunchenko, A.S., (2018). Optimal Design of the Shiryaev-Roberts Chart: Give Your Shiryaev-Roberts a Headstar, *Frontiers in Statistical Quality Control*, 12, 65-86.
- [24] Pollak, M. & Siegmund, D. (1985). On robustness of the Shiryaev–Roberts change-point detection procedure under parameter misspecification in the post-change distribution, *Communications in Statistics - Theory and Methods*, 72(2), 2185-2206.
- [25] Wen Y., Wu J., Zhou Q., & Tseng T., (2019). Multiple-Change-Point Modeling and Exact Bayesian Inference of Degradation Signal for Prognostic Improvement, *IEEE Trans. on Auto. Sci and Eng.*, 16(2), 613-628.
- [26] Nath S., Wu J., (2018). Bayesian Quickest Change Point Detection with Multiple Candidates of Post-Change Models, *IEEE Global Conf. on Signal and Information Processing*, 26-29 Nov, Anaheim, USA.
- [27] Geng J., & Lai L., (2013). Bayesian Quickest change point detection and localization in sensor networks, *IEEE Global Conf. on Signal and Information Processing*, 3-5 Dec., Austin TX, USA.
- [28] Adams, R. P., & MacKay, D. J., (2007). Bayesian online change point detection, *ArXivPrepr. ArXiv:0710.3742*.
- [29] Saatçi, Y., Turner, R. D., & Rasmussen, C. E. (2010). Gaussian process change point models, *Proceedings of the 27th Int'l Conf. on Mach. Learn. (ICML-10)*, 10, 927–934.
- [30] Carlin, B. P., Gelfand, A. E., & Smith, A. F. M. (1992). Hierarchical Bayesian Analysis of Changepoint Problems, *J. R. Stat. Soc. Ser. C Appl. Stat.*, 41(2), 389–405.
- [31] Loschi, R. H. & Cruz, F. R. B. (2005). Bayesian identification of multiple change points in poisson data, *Adv. Complex Syst.*, 08(4), 465–482.

- [32] Yao, Y.-C. (1988). Estimating the number of change-points via Schwarz' criterion," *Stat. Probab. Lett.*, 6(3), 181–189.
- [33] Whiteley, N., Andrieu, C. & Doucet, A. (2011). Bayesian computational methods for inference in multiple change-points models, submitted for publication.
- [34] Ruggieri, E., & Antonellis, M. (2016). An exact approach to Bayesian sequential change point detection, *Comput. Stat. Data Anal.*, 97, 71–86.
- [35] Chopin, N. (2007). Dynamic Detection of Change Points in Long Time Series, *Ann. Inst. Stat. Math.*, 59(2), 349–366.
- [36] Barry, D., & Hartigan, J. A., (1993). A Bayesian Analysis for Change Point Problems, *J. Am. Stat. Assoc.*, 88(421), 309–319.
- [37] Hinkley, D. V. (1970). Inference About the Change-Point in a Sequence of Random Variables, *Biometrika*, 57(1), 1–17.
- [38] Hinkley, D. V. (1972). Time-Ordered Classification, *Biometrika*, 59(3), 509–523.
- [39] Joseph, L. & Wolfson, D. B. (1992). Estimation in multi-path change-point problems, *Commun. Stat. - Theory Methods*, 21(4), 897–913.
- [40] Zou, C., Liu, Y., Qin, P., & Wang, Z. (2007). Empirical likelihood ratio test for the change-point problem, *Stat. Probab. Lett.*, 77(4), 374–382.
- [41] Diop M.L., & Kengne W., (2020). Poisson QMLE for change-point detection in general integer-valued series, *arxiv.org*, doi: <https://doi.org/10.48550/arXiv.2007.13858>.
- [42] Bai, J. (2000). Vector autoregressive models with structural changes in regression coefficients and in variance-covariance matrices, *Ann. Econ. Finance*, 1(2), 303-339.
- [43] Geng J., Zhang B., Huie L.M., & Lai L., (2019). Online Change-Point Detection of Linear Regression Models, *IEEE Trans. on Signal Processing*, 67(12), 3316–3329.
- [44] Loschi R., Pontel J.G., & Cruz F.R.B., (2010). Multiple Change -Point Analysis for Linear Regression Models, *Chilean Journal of Statistics*, 1(2), 93-112.
- [45] Brown, R.L., Durbin, J., & Evans, J. M., (1975). Techniques for Testing the Constancy of Regression Relationships over Time, *J. R. Stat. Soc. Ser. B Methodol.*, 37(2), 149–192.
- [46] Bai, J. (1997). Estimation of a Change Point in Multiple Regression Models, *Rev. Econ. Stat.*, 79(4), 551–563.
- [47] Jandhyala, V. K., & MacNeill, I. B. (1991), Tests for parameter changes at unknown times in linear regression models, *J. Stat. Plan. Inference*, 27(3), 291–316.
- [48] Gurevich, G., & Vexler, A. (2005). Change point problems in the model of logistic regression, *J. Stat. Plan. Inference*, 131(2), 313–331.
- [49] Preminger, A., & Wettstein, D. (2005). Using the Penalized Likelihood Method for Model Selection with Nuisance Parameters Present only under the Alternative: An Application to Switching Regression Models, *J. Time Ser. Anal.*, 26(5), 715–741.
- [50] Winkler, S. Affenzeller, M., Kronberger, G., Kommenda, M., Burlacu, B., & Wagner, S. (2015). Sliding Window Symbolic Regression for Detecting Changes of System Dynamics, in *Genetic Programming Theory and Practice XII*, Springer, Cham, 91–107.
- [51] Bandettini, P.A., Jesmanowicz, A., Wong, E. C., & Hyde, J. S. (1993). Processing strategies for time-course data sets in functional mri of the human brain, *Magn. Reson. Med.*, 30(2), 161–173.
- [52] Xiong, J., Gao, J.-H., Lancaster, J. L., & Fox, P. T. (1996). Assessment and optimization of functional MRI analyses, *Hum. Brain Mapp.*, 4(3), 153–167.
- [53] Hossein-Zadeh, G. A., Ardekani, B. A., & Soltanian-Zadeh, H. (2003). Activation detection in fMRI using a maximum energy ratio statistic obtained by adaptive spatial filtering, *IEEE Trans. Med. Img.*, 22(7), 795–805.
- [54] Roche, A., Lahaye, P. J., & Poline, J. B. (2004). Incremental activation detection in fMRI series using Kalman filtering, *2nd IEEE Int'l Symp. on Biomedical Imaging: Nano to Macro (IEEE Cat No. 04EX821)*, Arlington, VA, USA, 1, 376–379.
- [55] M. Singh, J. J. L. Al-Dayeh, Kim, T., & P. Colletti, (1999). Cross-correlation technique to identify activated pixels in a three-condition fMRI task, *IEEE Trans. Nucl. Sci.*, 46(3), 520–526.
- [56] Ruttimann, U. E., & Unser M., Rawlings, R.R., Rio, D., Ramsey, N.F., Mattay, V.S., Hommer, D.W., Frank, J.A., Weinberger, D.R. (1998). Statistical analysis of functional MRI data in the wavelet domain, *IEEE Trans. Med. Imaging*, 17(2), 142–154.
- [57] Lai, S.-H. & Fang, M., (1999). A novel local PCA-Based method for detecting activation signals in fMRI, *Magn. Reson. Imaging*, 17(6), 827–836.

- [58] Tzikas, D. G., Likas, A., Galatsanos, N. P., Lukic, A. S. & Wernick, M. N. (2004). Bayesian regression of functional neuroimages, *12th European Signal Proc. Conf.*, Vienna, Austria, 801–804.
- [59] Ferreira da Silva, A. R. (2011). A Bayesian multilevel model for fMRI data analysis, *Comput. Meth. Prog Biomed.*, 102(3), 238–252.
- [60] Akhbari, M., Babaie-Zadeh, M., Fatemizadeh, E. & Jutten, C., (2010). An entropy based method for activation detection of functional MRI data using Independent Component Analysis, *IEEE Int'l Conf. on Acoustics, Speech and Signal Processing*, Dallas, TX, USA, 2014–2017.
- [61] Tang, X., Zeng, W., Shi, Y., & Zhao, L. (2018). Brain activation detection by modified neighborhood one-class SVM on fMRI data, *Biomed. Signal Process. Control*, 39(Supp. C), 448–458.
- [62] Efron, B., Hastie, T., Johnstone, I. & Tibshirani, R. (2004). Least Angle Regression, *Ann. Stat.*, 32(2), 407–499
- [63] Friston, K. J., Jezzard, P. & Turner, R., (1994). Analysis of functional MRI time-series, *Hum. Brain Mapp.*, 1(2), 153–171
- [64] Friston, K. J., Holmes, A.P., Poline, J.B., Grasby, P.J., Williams, S.C., Frackowiak, R.S., & Turner, R. (1995) Analysis of fMRI Time-Series Revisited, *NeuroImage*, 2(1), 45–53
- [65] Robinson, L. F., Wager, T. D., & Lindquist, M. A. (2010). Change point estimation in multi-subject fMRI studies, *NeuroImage*, 49(2), 1581–1592.
- [66] Lindquist, M. A., Waugh, C., & Wager, T. D. (2007). Modeling state-related fMRI activity using change-point theory, *NeuroImage*, 35(3), 1125–1141.
- [67] Barnett, I. & Onnela, J.-P. (2016). Change Point Detection in Correlation Networks, *Sci. Rep.*, 6, 18893.
- [68] Gorgolewski, K. J., Storkey, A., Bastin, M.E., Whittle, I.R., Wardlaw, J.M., & Pernet, C.R. (2013). A test-retest fMRI dataset for motor, language and spatial attention functions, *GigaScience*, 2(1), 6
- [69] Friston, K. J., Frith, C. D., Frackowiak, R. S. J. & Turner, R., (1995). Characterizing Dynamic Brain Responses with fMRI: A Multivariate Approach, *NeuroImage*, 2(2 Part A): 166–172.
- [70] Collignon, A., Maes, F., Delaere, D., Vandermeulen, D., Suetens, P. & Marchal, G., (2015). Automated multi-modality image registration based on information theory, *Compt. Imag. and Vis.*, 3, 263–274.
- [71] Evans, A. C., Collins, D. L., Mills, S. R., Brown, E. D., Kelly, R.L. & Peters, T. M. (1993). 3D statistical neuroanatomical models from 305 MRI volumes, *IEEE Nucl. Sci. Symp. and Med. Imag. Conf.*, San Francisco, CA, USA, 3, 813–1817.
- [72] Ebner, N. C., Riediger, M., & Lindenberger, U., (2010). FACES--a database of facial expressions in young, middle-aged, and older women and men: development and validation, *Behav. Res. Methods*, 42(1), 351–362.
- [73] Grubbs, F. E., (1969). Procedures for Detecting Outlying Observations in Samples, *Technometrics*, 11(1), 1–21.
- [74] Candemir, C., (2018). Change Point Estimation in Multi Subject Social Support fMRI Studies, PhD Thesis, Int'l Computer Institute, Ege University, Izmir, Turkey.